I/P Transducer Application of Model-Based Wear Detection and Estimation using Steady State Conditions

Christopher Teubert[1] and Matthew Daigle[2]

[1] *SGT, Inc. NASA Ames Research Center, Moffett Field, CA, 94035, USA*
christopher.a.teubert@nasa.gov

[2] *NASA Ames Research Center, Moffett Field, CA, 94035, USA*
matthew.j.daigle@nasa.gov

ABSTRACT

For modern systems, wear estimation plays an important role in preventing failure, scheduling maintenance, and improving utility. Wear estimation relies on a series of sensors, measuring the state of the system. In some components, the sensors used to estimate wear may not be fast enough to capture brief transient states that are indicative of wear. For this reason it is beneficial to be capable of detecting and estimating the extent of component wear using steady-state measurements. This paper details a method for estimating component wear using steady-state measurements, and describes a case study of a current/pressure (I/P) transducer. I/P Transducer nominal and off-nominal behavior are characterized using a physics-based model, and validated against expected component behavior. This model is used to determine steady state responses to many common I/P Transducer wear modes, isolate the active wear mode, and estimate its magnitude.

1. INTRODUCTION

As systems are becoming more complex, more expensive, and are being sent to increasingly unreachable places, such as space or the bottom of the ocean, wear detection and estimation become increasingly important. Wear detection and estimation play a critical role in preventing failure, scheduling maintenance, and improving system utility.

Many modern wear estimation techniques rely on measurement of the system's transient states (Daigle & Goebel, 2013; Orchard & Vachtsevanos, 2009; Saha & Goebel, 2009; Luo, Pattipati, Qiao, & Chigusa, 2008). However, in some components, the available sensors may not be fast enough to capture brief transient states that are indicative of wear. This can either be a result of sensor technological limits, or budgetary

constraints on sensor selection (as sensors with higher resolution and higher sampling frequencies are generally more expensive). For this reason, it is beneficial to be capable of detecting and estimating the extent of component wear using only steady-state measurements. Previous work in prognostics does not address this need, and a new methodology is required.

This paper describes a method for estimating component wear from steady-state conditions. This is accomplished utilizing a physics-based model that accounts for system behavior in both nominal and degraded conditions, and that is tuned utilizing physical specifications and knowledge of system behavior. This model is then used to map the effect of various modes of wear on steady-state behavior. Combined with a particle filter-based estimation scheme, this model can be used for prognostics, as described in previous work by (Daigle & Goebel, 2011; Orchard & Vachtsevanos, 2009; Saha & Goebel, 2009; Zio & Peloni, 2011).

As a case study, this method is applied to a current/pressure transducer, henceforth referred to as an I/P Transducer or IPT. I/P Transducers are effectively pressure regulators that vary the output pressure depending on the supplied electrical current signal. They operate by throttling a nozzle to create a pressure difference across a diaphragm, which controls the throttling of a valve. These are often used for supplying precise pressures to control pneumatic actuators and valves.

The paper is organized as follows. The development of the IPT model is described in Section 2. Section 3 details the process of mapping IPT wear from steady state conditions, and using that mapping to detect and estimate wear in physical systems. The paper concludes with a discussion of the implications of this research and a description of future work in Section 4.
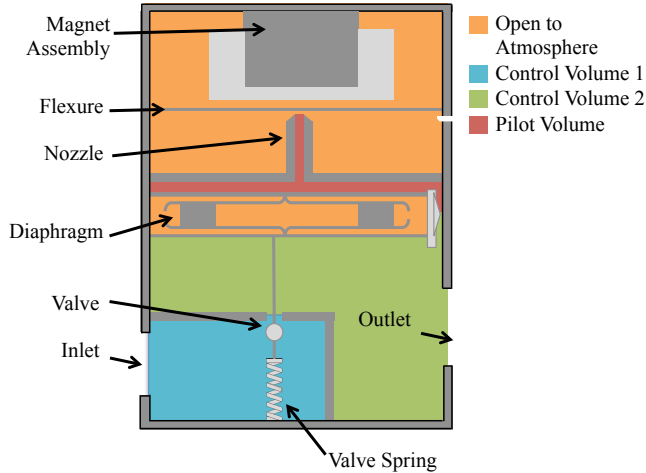
Figure 1. Current/Pressure Transducer Schematic

Table 1. IPT Specifications

Name	Type 1000 IPT
Manufacturer	Marsh Bellofram
Supply Pressure Range	18-100 psig
Input Signal Range	4-20 mA
Output Pressure Range	3-15 psig

2. I/P TRANSDUCER MODELING

In this section, we develop a physics-based model of both healthy and faulty IPT behavior. This is used to identify how faulty behavior affects performance for development of the wear detection and estimation methodology, and for possible future prognostic applications. This model was created using domain knowledge of the system's behavior and physical make-up.

As a case study, we use a Marsh Bellofram Type 1000 IPT, illustrated in Figures 1 and 2. This model was chosen because of its use in the pneumatic valve testbed at NASA Ames Research Center (Kulkarni, Daigle, & Goebel, 2013). The IPT is divided into three distinct control volumes (CVs), each marked in a different color in the image. The IPT output pressure varies with the current supplied to the magnet assembly. When the current is high, the magnet assembly throttles the flow out of the pilot nozzle, allowing less air to escape. With a low input current more gas escapes from the nozzle, lowering the pilot pressure. The pressure difference across the diaphragm moves the valve, which adjusts the gas flow between CV1 and CV2. Adjusting this flow changes the pressure in CV2 and in the outlet. Some specifications for this IPT are included in Table 1 (Marsh Bellofram, n.d.).

In this section we will describe development, configuration, validation, and use of the IPT model for both the nominal and

Figure 2. Current/Pressure Transducer

wear conditions.

2.1. Problem Formulation

We assume the system may be described by

$$\dot{\mathbf{x}}(t) = \mathbf{f}(t, \mathbf{x}(t), \boldsymbol{\theta}(t), \mathbf{u}(t), \mathbf{v}(t)) \tag{1}$$

$$\mathbf{y}(t) = \mathbf{h}(t, \mathbf{x}(t), \boldsymbol{\theta}(t), \mathbf{u}(t), \mathbf{n}(t)) \tag{2}$$

where $t \in \mathbb{R}$ is the continuous time variable, $\mathbf{x}(t) \in \mathbb{R}^{n_x}$ is the state vector, $\theta(\mathbf{t}) \in \mathbb{R}^{n_\theta}$ is the parameter vector, $\mathbf{u}(t) \in \mathbb{R}^{n_u}$ is the input vector, $\mathbf{v}(t) \in \mathbb{R}^{n_v}$ is the process noise vector, $\mathbf{f}$ is the state equation, $\mathbf{y}(t) \in \mathbb{R}^{n_y}$ is the output vector, $\mathbf{n}(t) \in \mathbb{R}^{n_n}$ is the measurement noise vector, and $\mathbf{h}$ is the output equation.

Given a system defined in this way, the objective is to estimate the wear parameter, $\theta_w \in \boldsymbol{\theta}$, given a measured steady state output, $\mathbf{y}_{SS}$, and a known input, $\mathbf{u}$. For this architecture it is assumed that only one mode of wear is occurring at a time (single fault assumption). It may be possible to estimate wear in the case of multiple simultaneous modes of wear, given additional steady state output measurements at other input currents. This is not under the scope of the current research, but will be explored in future research.

2.2. Nominal Model

The IPT model was developed using mass and energy balances. Each CV contains gas at a specific pressure, changing depending on the gas in-flow and out-flow. The system's state is signified by the vector $\mathbf{x}(t)$, consisting of the pressures at each control volume $(p_1(t), p_2(t), p_{pilot}(t))$, the position and velocity of the valve ($x_V(t)$ and $v_V(t)$, respectively), and the flexure position and velocity ($x_F(t)$ and $v_F(t)$, respectively).

The IPT performance is dependent on the supply pressure provided at the inlet, $p_i(t)$, and the signal current sent to the magnet assembly, $i(t)$. These two values make up the input vector, $\mathbf{u}(t)$. For the IPT being modeled, the signal current is between 4 and 20 mA, which varies the outlet pressure, $p_{out}(t)$, between 3–15 PSIG. Outlet pressure is considered to be the only value in the output vector, $\mathbf{y}(t)$.

The input ($\mathbf{u}(t)$), state ($\mathbf{x}(t)$), state derivative ($\dot{\mathbf{x}}(t)$) and output ($\mathbf{y}(t)$) vectors are summarized below:

$$\mathbf{u}(t) = \begin{bmatrix} p_i(t) \\ i(t) \end{bmatrix} \tag{3}$$

$$\mathbf{x}(t) = \begin{bmatrix} p_1(t) \\ p_2(t) \\ p_{pilot}(t) \\ p_{out}(t) \\ x_V(t) \\ v_V(t) \\ x_F(t) \\ v_F(t) \end{bmatrix} \tag{4}$$

$$\dot{\mathbf{x}}(t) = \begin{bmatrix} \dot{p}_1(t) \\ \dot{p}_2(t) \\ \dot{p}_{pilot}(t) \\ \dot{p}_{out}(t) \\ v_V(t) \\ a_V(t) \\ v_F(t) \\ a_F(t) \end{bmatrix} \tag{5}$$

$$\mathbf{y}(t) = p_{out}(t) \tag{6}$$

Here velocity, v, and acceleration, a, are defined as the derivative of position, x, and velocity, respectively. Additionally gas flow into a control volume from a bordering control volume is represented by $\dot{q}_{ij}$, where the subscript i represents the first control volume and j the bordering one and $\dot{q}_{ij}$ is the fluid flow into i from j. The flow, $\dot{q}_{ij}$, is a function of the pressure in the control volume, p_i, pressure in the second control volume, p_j, and the area of the opening between them, A_{ij}. These equations are summarized below:

$$\dot{x} = v \tag{7}$$
$$\dot{v} = a \tag{8}$$
$$\dot{q}_{ij} = A_{ij}\sqrt{|p_i - p_j|} * sgn(p_i - p_j) \tag{9}$$

Each of the $\dot{p}$ terms are dependent on the bordering control volumes. The sum over all the interactions with a given control volume gives the total pressure flux. Accounting for all the bordering CVs the $\dot{p}$ equations become

$$\dot{p}_1 = (\dot{q}_{12} + \dot{q}_{10})\frac{R * T_1}{V_1} \tag{10}$$

$$\dot{p}_2 = (\dot{q}_{21} + \dot{q}_{2p} + \dot{q}_{2Out})\frac{R * T_2}{V_2} \tag{11}$$

$$\dot{p}_p = (\dot{q}_{p2} + \dot{q}_{pNozzle})\frac{R * T_p}{V_p} \tag{12}$$

$$\dot{p}_{out} = \dot{q}_{out2}\frac{R * T_{out}}{V_{out}} \tag{13}$$

where R represents the gas constant, and T the temperature in that control volume.

The signal current is supplied to the magnet assembly, which reacts, applying pressure on the flexure. This pressure is greater for greater signal currents. As the flexure stretches, it throttles the airflow out of the nozzle. For low input signals, the flexure flexes less, allowing more air to escape from the pilot volume, decreasing its pressure. The pilot volume is supplied from CV_2 by a small entry to the right of the diaphragm as seen in Figure 1. The net force on the flexure is the sum of the magnet assembly force (F_{Mag}), the resistive force of the Flexure (F_{Flex}), and friction ($F_{Friction}$):

$$F_F = F_{Mag} + F_{Flex} + F_{Friction}. \tag{14}$$

where the individual forces are

$$F_{Mag} = \frac{i^2}{2}(C_{mag} - C_{mag2} * r_{mag}) \tag{15}$$

$$F_{Flex} = -k_{Flex}(x_F - x_{F0}) \tag{16}$$

$$F_{Friction} = C_f v_F \tag{17}$$

Here the lumped parameters C_{mag} and C_{mag2} include the gap between the coils and the metal, the area of the metal, the number of turns of the coil, and the magnetic constant. The coil resistance is represented by r_{mag}. Here the value C_f is the coefficient of friction.

The pressure difference between CV_2 and CV_{pilot} produces a closing force on the valve. The lower the input signal the greater the closing force. The net force on the valve (F_V) is the sum of the forces of the Valve Spring (F_{VS}), the force from the pressure difference across the valve (F_{PD}), the force created by the pressure difference across the Diaphragm ($F_{Diaphragm}$), and the force of friction ($F_{Friction}$). The throttling of this valve changes the flow rate between CV_1 and CV_2, affecting the output pressure P_{out}.

$$F_V = F_{VS} + F_{PD} + F_{Diaphragm} + F_{Friction} \tag{18}$$

(a) Outlet Pressure, P_{out}
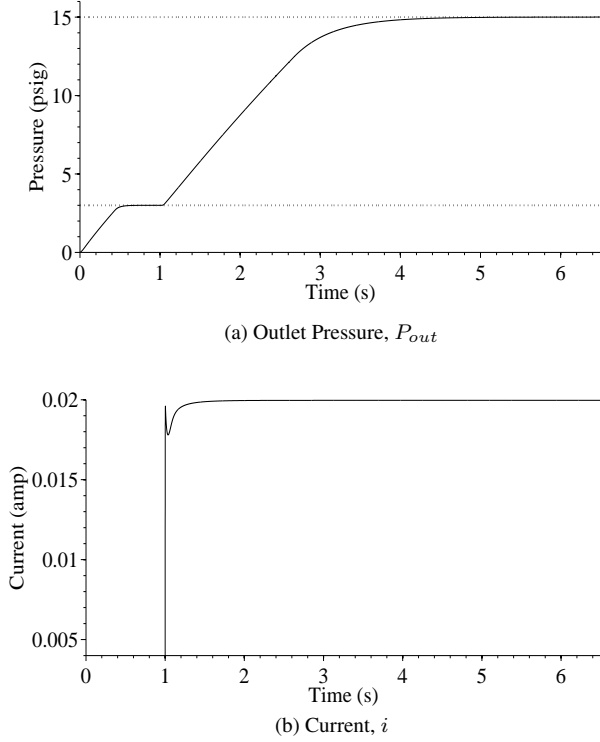
(b) Current, i

Figure 3. Outlet pressure for different currents

where the individual forces are

$$F_{VS} = -k_V * (x_V - x_{V0}) \qquad (19)$$
$$F_{FD} = (p_2 - p_1) * A_V \qquad (20)$$
$$F_{Diaphragm} = (p_{Pilot} - p_2) * A_D \qquad (21)$$
$$F_{Friction} = C_f v_V \qquad (22)$$

where A_V and A_D are the areas of the valve and the diaphragm, respectively, and k_V is the valve spring coefficient.

Each of these relationships were then converted to be in terms of acceleration using the following relationship

$$a_V = \frac{1}{m_V} F_V \qquad (23)$$
$$a_F = \frac{1}{m_F} F_F \qquad (24)$$

where m_V and m_F are the mass of the valve and flexure, respectively.

The movement of both the flexure and the valve are derived by integrating their respective acceleration equations. The nominal output pressure response is illustrated in Figure 3a, with its respective signal current in Figure 3b.

This IPT model was qualitatively validated by comparing the simulated behavior with known behavior. This domain knowledge was gathered from system documentation, con-

versations with the manufacturing company, and observations of actual behavior.

2.3. Wear Model

Through discussions with the manufacturers and with users of I/P transducers and similar components, five possible wear modes were indicated. These wear modes are described below:

1. **Inlet Leak** A leak where the supply pressure is provided to CV_1. Modeled by adding a leak of area A_{in} for fluid flow between CV_1 and the surrounding environment (at 1 atm). The resulting fluid flow is represented by

$$\dot{q}_{in} = A_{in} \sqrt{|p_1 - p_{atm}|} * sgn(p_1 - p_{atm}) \qquad (25)$$

2. **Valve Seat Leak** A leak between CV_1 and CV_2. Modeled by adding a leak of area A_{VS} for fluid flow between CV_1 and CV_2. A negative A_{VS} models clogging of the valve.

$$\dot{q}_{VS} = A_{VS} \sqrt{|p_1 - p_2|} * sgn(p_1 - p_2) \qquad (26)$$

3. **Outlet Leak** A leak at the outlet. Modeled by adding a leak of area A_{out} for fluid flow between CV_2 and the surrounding environment (at 1 atm).

$$\dot{q}_{out} = A_{out} \sqrt{|p_2 - p_{atm}|} * sgn(p_2 - p_{atm}) \qquad (27)$$

4. **Valve Spring Weakening** A weakening of the valve spring. Modeled by decreasing the spring coefficient, k_V.

5. **Magnet Assembly Weakening** A weakening of the magnet assembly. Modeled by increasing the resistance in the magnet coils, r_{mag}.

The wear parameters vector, $\boldsymbol{\theta_w}$, consisting of values representing the state of wear for each of the five wear modes, is shown in the below equation

$$\boldsymbol{\theta_w} = \begin{bmatrix} A_{in} \\ A_{VS} \\ A_{out} \\ k_V \\ r_{mag} \end{bmatrix} \qquad (28)$$

3. WEAR ESTIMATION

Wear estimation is the process of estimating the current extent of wear on a system. This is important for prognostics (predicting failure), scheduling maintenance, and triggering automated mitigation actions. This is often done using methods such as a Kalman Filter or Particle Filter (Arulampalam, Maskell, Gordon, & Clapp, 2002; Daigle, Saha, & Goebel, 2013).

4

A lookup table method was used for fault estimation. This method was chosen because of its fast, efficient nature and its ability to be applied to both linear and non-linear systems. To define this lookup table the I/P transducer was simulated at various states of each wear mode and various input currents. The steady state output pressure was recorded for each case. The result was used as a reverse lookup table to estimate the wear given a specific observed steady state output pressure for a given input current. Values between data points were linearly interpolated. This was found to be sufficiently accurate given a high granularity lookup table. The granularity of the lookup table can be adjusted to increase accuracy as needed.

The resulting outlet pressure for each fault mode given a high and low input current can be seen in Figure 4. Here the outlet pressure given a high input current is indicated by the green dashed line, while that based on a low current is indicated by the blue solid line. All possible values for the IPT at a given fault level fall between these two points. In this case it was found that monitoring the steady state output pressure does not allow for the estimation of the damage state in the case of an inlet leak. This leak results in a decrease in the pressure in CV_1, which does not result in a change in the output pressure until a much larger leak (around 0.2 m^2). For this reason the Inlet Leak case has not been included in the figures.

By contrast, the valve seat leak has a definite increasing effect on the outlet pressure (Figure 4a). This change in output pressure is a result of additional gas coming into CV_2 from CV_1 through the leak opening. For a leak of 0.005 m^2 the outlet pressure increased by 0.11 psig for a high signal current and 0.022 psig for a low current.

The outlet leak also has a definite and measurable effect on the outlet pressure. As the leak grows in size, more gas escapes from CV_2, resulting in a lower outlet pressure as seen in Figure 4b. For a leak of 0.01 m^2 the outlet pressure decreases by 0.05 psig for a high signal current and 0.0045 psig for a low current.

The valve spring exerts a force on the valve system countering that of the diaphragm. As the spring wears, the spring coefficient, k, decreases. This results in a lower counter force against the diaphragm, causing an increased output pressure as the spring coefficient decreases, as seen in Figure 4c. The effect of this is much more prominent for high input current, where the force of the diaphragm is higher. For a weakening of 0.005 to a k of 3.212 N/m the outlet pressure increased by 0.29 psig for a high signal current and remained the same for a low current.

Finally, wear in the magnet-coil assembly is simulated here by increasing the coil resistance. This, in turn, reduces the force of the magnet on the flexure proportionally with input current. The decreased force results in a greater pressure dif-

ference across the diaphragm. This closes the valve, and results in a decreased output pressure as seen in Figure 4d. This effect is much almost unseen for the low input current as a result of how the effect scales with current. For an increase of 0.1 Ω to a r_{Mag} of 180.1 Ω the outlet pressure decreased by 0.045 psig for a high signal current and remained the same for a low current.

Each of these four wear modes resulted in a change in outlet pressure. The results for single point wear have been summarized in Table 2.

Table 2. Affect of Wear Modes on Outlet Pressure

Wear Mode	Effect
Inlet Leak	None
Valve Seat Leak	Increased Outlet Pressure
Outlet Leak	Decreased Outlet Pressure
Worn Spring	Increased Outlet Pressure
Work Coil	Decreased Outlet Pressure

Once the relationship between the fault parameter (θ), input current (i), and the measured steady state output ($\mathbf{y}_{SS}$) has been determined the resulting knowledge base can be used for wear isolation and estimation.

Two measurements with two different input current levels are required to completely isolate the fault cause. This is to differentiate between two faults that result in the same effect on output pressure. For example, if the outlet pressure is measured to be higher than it should be, that could either be indicative of a worn spring or a valve seat leak. Each of these leaks has a different relationship with input current. The second measurement allows for isolation between similar such faults. For systems with additional fault modes additional measurements may be needed to isolate between similar faults.

The following section details an example of this method.

3.1. Example

For this example let us assume we have a leak in the valve seat of 0.001 m^2.

The first measurement of steady state outlet pressure is 15.0215 psig at the maximum signal current of 20 mA. Using the reverse lookup table there are two possible options: a leak in the valve seat of 0.0098 m^2, or worn spring with a spring constant of 3.2167 N/m (down 0.0003).

To definitely isolate the wear mode a second measurement is taken, this time with the minimum signal current of 4 mA. The outlet pressure is measured to be 3.0044 psig. This can either correspond to a leak in the valve seat of 0.0105 m^2, or worn spring with a spring constant of 3.173 N/m (down 0.044).
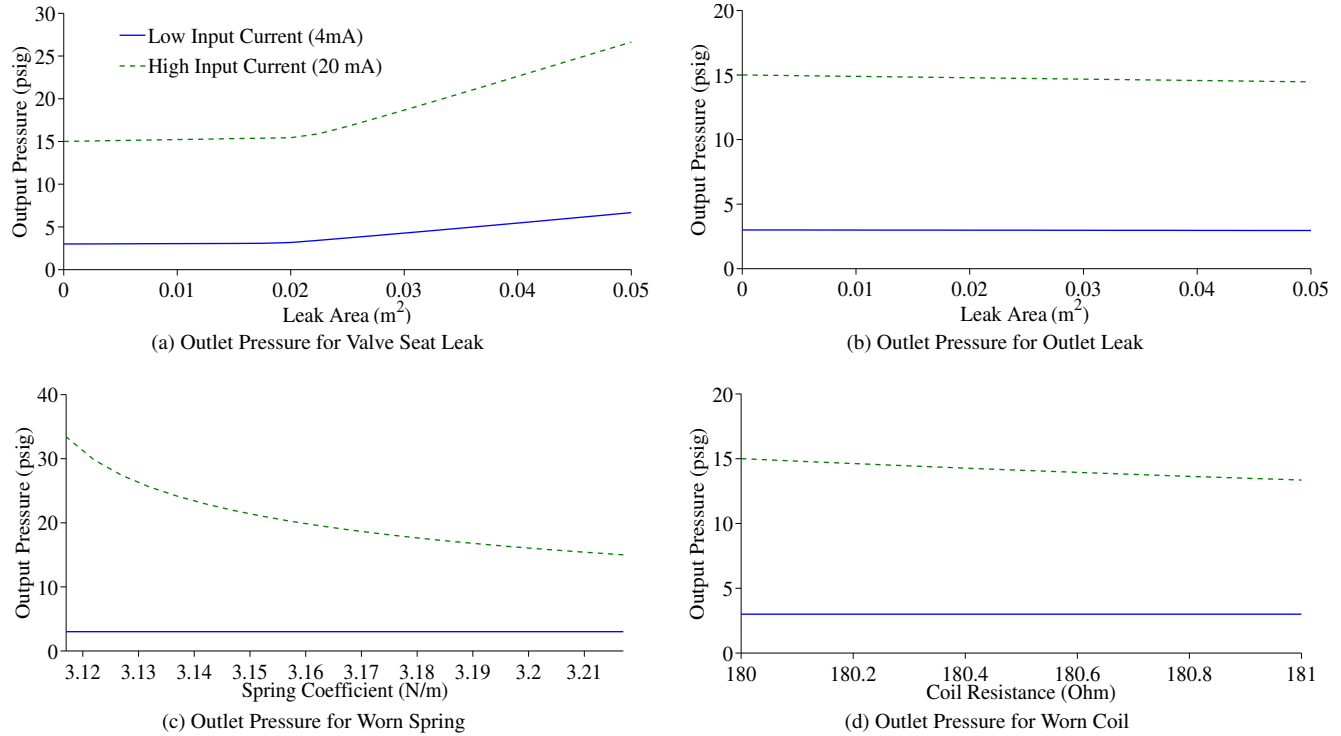
Figure 4. Damaged Outlet Pressure

Both measurements result in a valve seat leak estimation that is fairly similar, allowing the user to estimate that there is a leak in the valve seat of around 0.01015 m^2. This is calculated by taking the average of the two estimates. The difference in these measurements is due to measurement noise ($\mathbf{n}$). Additional measurements at different input currents could be used to further refine the damage estimate, and filter out system noise.

4. CONCLUSION

This paper details the development of a model-based wear estimation approach using steady state measurements of the outlet pressure of a current/pressure transducer. This approach was then applied for the wear modes of Inlet leaks, Valve Seat Leaks, Outlet Leaks, Spring Wear, and Coil Wear, which were determined to be the most likely modes of failure.

This method was shown to be effective in identifying wear in simulations for a worn coil, worn spring, outlet leak, and leak in the valve seat. With each of these wear modes the resulting effect on the outlet pressure was different when considering two different input currents. Measuring the outlet pressure at two different input currents allows for the identification of the failure mode. The lookup table created in this study can then be used to estimate the severity of the wear. The results here demonstrate the effectiveness of steady state wear estimation

for an I/P transducer.

This approach to wear estimation allows for wear estimation for components where sensors may not be fast enough to capture brief transient states that are indicative of wear. The results from wear estimation routines such as this one can then be used to create a prognostic model, schedule maintenance, or trigger automated mitigation action.

This study relied on physics-based simulations of IPT behavior validated against observations of actual system behavior. We are currently in the process of constructing a testbed that will include the IPT modeled for this study (Kulkarni et al., 2013). Future work includes testing this method of wear estimation in this testbed. Additionally, future work includes the application of prognostics utilizing wear estimation, estimation of multiple simultaneous wear modes, and uncertainty in wear estimation from steady state conditions.

gram.

NOMENCLATURE

a	Acceleration
A	Area
C_f	Coefficient of Friction
C_{mag}	Magnetic Lumped Parameter
$\mathbf{f}$	State Equation
F	Force
$\mathbf{h}$	Output Equation
i	Current
k	Spring Constant
m	Mass
$\mathbf{n}$	Sensor Noise Vector
p	Pressure
r_{mag}	Magnetic Coil Resistance
R	Gas Constant
t	Time, continuous
T	Temperature
$\mathbf{u}$	Input Vector
w	Wear Parameter
$\mathbf{w}$	Wear Parameter Vector
x	Position
$\mathbf{x}$	State Vector
v	velocity
$\mathbf{v}$	Process Noise Vector
$\mathbf{y}$	Output Vector
$\boldsymbol{\theta}$	Parameter Vector

REFERENCES

Arulampalam, M. S., Maskell, S., Gordon, N., & Clapp, T. (2002). A tutorial on particle filters for on-line nonlinear/non-Gaussian Bayesian tracking. *IEEE Transactions on Signal Processing*, *50*(2), 174–188.

Daigle, M., & Goebel, K. (2011, August). A model-based prognostics approach applied to pneumatic valves. *International Journal of Prognostics and Health Management*, *2*(2).

Daigle, M., & Goebel, K. (2013, May). Model-based prognostics with concurrent damage progression processes. *IEEE Transactions on Systems, Man, and Cybernetics: Systems*, *43*(4), 535-546.

Daigle, M., Saha, B., & Goebel, K. (2012, March). A comparison of filter-based approaches for model-based prognostics. In *Proceedings of the ieee aerospace conference.*

Kulkarni, C., Daigle, M., & Goebel, K. (2013, September). Implementation of prognostic methodologies to cryogenic propellant loading testbed. *Proceedings of 2013 IEEE Autotestcon.*

Luo, J., Pattipati, K. R., Qiao, L., & Chigusa, S. (2008, September). Model-based prognostic techniques applied to a suspension system. *IEEE Transactions on Systems, Man and Cybernetics, Part A: Systems and Humans*, *38*(5), 1156 -1168.

Marsh Bellofram. (n.d.). Type 1000 i/p & e/p transducers [Computer software manual].

Orchard, M., & Vachtsevanos, G. (2009, June). A particle filtering approach for on-line fault diagnosis and failure prognosis. *Transactions of the Institute of Measurement and Control*(3-4), 221-246.

Saha, B., & Goebel, K. (2009, September). Modeling Li-ion battery capacity depletion in a particle filtering framework. In *Proceedings of the annual conference of the prognostics and health management society 2009.*

Zio, E., & Peloni, G. (2011). Particle filtering prognostic estimation of the remaining useful life of nonlinear components. *Reliability Engineering & System Safety*, *96*(3), 403-409.

BIOGRAPHIES

Christopher Teubert received his B.S. in Aerospace Engineering from Iowa State University in 2012. While at Iowa State University, he conducted research on asteroid deflection mission design and asteroid fragment propagation for Iowa State University's Asteroid Deflection Research Center (ADRC). Previous to his current position he worked as a spacecraft systems engineer for a Mars sample return mission as part of the NASA Academy Program. He is currently researching systems and algorithms for diagnostics, prognostics, and system health management for Stinger Ghaffarian Technologies, Inc. at NASA Ames Research Center's Prognostic Center of Excellence (PCoE). He plans to begin pursuing a M.S. in 2014.

Matthew Daigle received the B.S. degree in Computer Science and Computer and Systems Engineering from Rensselaer Polytechnic Institute, Troy, NY, in 2004, and the M.S. and Ph.D. degrees in Computer Science from Vanderbilt University, Nashville, TN, in 2006 and 2008, respectively. From September 2004 to May 2008, he was a Graduate Research Assistant with the Institute for Software Integrated Systems and Department of Electrical Engineering and Computer Science, Vanderbilt University, Nashville, TN. From June 2008 to December 2011, he was an Associate Scientist with the University of California, Santa Cruz, at NASA Ames Research Center. Since January 2012, he has been with NASA Ames Research Center as a Research Computer Scientist. His current research interests include physics-based modeling, model-based diagnosis and prognosis, simulation, and hybrid systems.